






Coconut shell biochar as a sustainable approach for nutrient removal from agricultural wastewater

Tivany Edwin¹⁾ , Puti Sri Komala^{*1)} , Mas Mera¹⁾ ,
Zulkarnaini Zulkarnaini¹⁾ , Zadariana Jamil²⁾ 

¹⁾ Andalas University, School of Engineering, Department of Environmental Engineering,
Limau Manis, Padang, Sumatera Barat 25163, Indonesia

²⁾ Faculty of Civil Engineering, Universiti Teknologi MARA, 40450 Shah Alam, Selangor, Malaysia

* Corresponding author

RECEIVED 07.11.2024

ACCEPTED 08.04.2025

AVAILABLE ONLINE 13.06.2025

Abstract: Coconut shell residues are abundant in tropical countries and have the potential to be further processed into biochar. Due to its specific characteristics, biochar has the potential to remove contaminants from wastewater. The intensification of agriculture in these tropical countries produces large volumes of wastewater that require nutrient removal before being discharged into water bodies. Accumulated nutrient in bodies of water can lead to eutrophication. This study investigates the capacity of coconut shell biochar in removing phosphate, ammonium, and nitrate from agricultural wastewater using both batch adsorption and fixed-bed column methods. The nutrient sorption capacity of biochar produced at different pyrolysis temperatures (300°C, 450°C, and 600°C) was evaluated and compared with locally produced biochar from Padang City. Findings indicated that the nutrient adsorption efficiency of coconut shell biochar is influenced by pyrolysis temperature and is comparable to that of local biochar. The sorption capacity of ammonium, nitrate, and phosphate using local biochar were 10.12, 7.51, and 10.79 mg·g⁻¹. A continuous sorption study using a fixed-bed column reactor confirmed the ability of local coconut shell biochar in removing nutrients from real agricultural wastewater. This study highlights the potential of utilising coconut shell waste as a sustainable material for nutrient removal from wastewater, thereby helping to prevent nutrient pollution in water bodies.

Keywords: agricultural wastewater, coconut shell biochar, nutrients, pyrolysis, sorption

INTRODUCTION

Population growth has been associated with an increase in intensive agricultural activities to meet food demand, which is closely associated with the use of synthetic fertilisers. These fertilisers contain several nutrients (ammonium, nitrate, and phosphate), not all of which are absorbed by plants. A portion of these nutrients is carried by agricultural runoff into water bodies. The risk of nutrient leaching is particularly high in intensively farmed regions of tropical countries. This runoff can lead to environmental issues, such as eutrophication, which adversely affect aquatic organisms as has been observed in several lakes in Indonesia (Edwin *et al.*, 2023a; Komala *et al.*, 2023). Therefore, agricultural wastewater should be treated prior being discharged

into water bodies (Rosemarin *et al.*, 2020) to prevent environmental contamination and negative ecological consequences.

Various methods, such as chemical precipitation and ion exchange, have been used to remove nutrients from wastewater. However, adsorption is recognised to be an effective method, particularly when using readily available adsorbents. Biochar, produced from agricultural waste, is one such cost-effective adsorbent. It is a high-carbon material produced through pyrolysis of biomass. The physicochemical characteristics of biochar depend on the raw materials used (Kumar and Bhattacharya, 2021). Agricultural waste like coconut shell is widely available in tropical areas. The local community produces biochar from coconut shells for various purposes, including grilling food, making it easily available in local markets.

Moreover, coconut shell biochar is mechanically durable and not easily broken.

This study was performed to analyse the sorption capacity of coconut shell biochar from aqueous solutions. It is also aimed to evaluate the effect of pyrolysis temperatures on the sorption capacity. The performance of locally produced biochar was compared with the pyrolysed coconut biochar using batch and continuous sorption in a fixed bed reactor. The results of this study are expected to provide insights into nutrient removal from agricultural wastewater, ensuring its safe discharge into the environment.

MATERIAL AND METHODS

PREPARATION AND PHYSICAL CHARACTERISTICS OF THE SORBENT MEDIA

Sorption experiments were conducted using batch method to evaluate the sorption capacity of coconut shell biochar to remove ammonium, nitrate, and phosphate from artificial wastewater. Initially, raw coconut shell biochar was cleaned and crushed to a particle size ~1 cm. The biochar was subjected to a controlled heating rate of 5°C per minute until the target pyrolysis temperature was reached, and then maintained for two hours. After pyrolysis, the biochar was allowed to cool naturally at room temperature, followed by thorough washing with distilled water to remove impurities. Once dried, the biochar was utilised in batch adsorption experiments to assess its sorption performance.

Coconut shells subjected to varied pyrolysis temperatures were collected as waste from local coconut milk shops, while locally produced coconut shell biochar was purchased from a traditional market. This study was performed in the laboratory using coconut shell biochar pyrolysed at three different temperatures: 300°C (CS300), 450°C (CS450), and 600°C (CS600). The sorption capacity of locally produced biochar (CST) was also assessed for comparison.

The surface morphology of biochar samples was examined using Scanning Electron Microscope coupled with Energy Dispersive X-ray (SEM-EDX), utilising Hitachi S-3400N model equipped with a Hitachi E-1045 ion sputter. Additionally, the functional groups present on the biochar were analysed using Fourier Transform Infrared (FTIR) (Perkin Elmer FT-IR spectrometer frontier L128-0099).

SORPTION OF NUTRIENTS USING BIOCHAR

For sorption experiments, artificial wastewater was prepared for each parameter using KNO₃ for nitrate, NH₄Cl for ammonium, and KH₂PO₄ for phosphate. Batch experiments were set up separately for each nutrient, with 0.5 g of biochar added to 100 cm³ of solution at varying contaminant concentrations of 10, 20, 40, and 80 mg·dm⁻³. Sorption capacity was assessed over different contact times of 1, 2, 3, 4, 5, and 6 h (Nguyen, 2015). During the experiments, the mixtures were continuously stirred at 180 rpm using an orbital shaker to ensure uniform contact. After each designated period, the solutions were filtered using filter paper for subsequent analysis.

Ammonium concentrations before and after the batch adsorption process were measured using the Nessler method at

a wavelength of 420 nm, while nitrate concentration analysis was performed using the cadmium reduction method, also at 420 nm. Phosphate levels were determined using the ascorbic acid method at a wavelength of 880 nm (APHA, 2003). These analytical techniques enabled precise evaluation of the biochar's sorption capacity for removing each nutrient contaminant, using Equation (1) (Tchobanoglous, Burton and Stensel, 2003):

$$q = \frac{(C_0 - C_t)V}{m} \quad (1)$$

where: q = sorption capacity (mg·g⁻¹), C_0 = initial nutrient concentration (mg·dm⁻³), C_t = nutrient concentration at time t (mg·dm⁻³), V = volume of the solution (dm³), and m = dry weight of biochar (g).

The maximum sorption capacity for each biochar is determined using the Langmuir equation (Eq. 3), which provides a quantitative measure of biochar's sorption efficiency under different condition.

SORPTION ISOTHERM AND KINETICS

Sorption isotherms were derived from the experimental data using different initial concentrations of nitrate, ammonium, and phosphate at 10, 20, 40, and 80 mg·dm⁻³. The solutions were stirred continuously at 180 rpm for 6 h to reach equilibrium. The resulting sorption isotherms were then analysed using the Freundlich isotherm model (Eq. 2) and the Langmuir isotherm model (Eq. 3) to evaluate the sorption characteristics and capacity of the biochar for each nutrient.

$$q_e = K_F(C_e)^{1/n} \quad (2)$$

where: q_e = quantity of nutrients adsorbed per gram of the adsorbent at equilibrium (mg·g⁻¹), K_F = Freundlich constant (dm³·g⁻¹), C_e = contaminant concentration at equilibrium (mg·dm⁻³), n = adsorption intensity constant (-).

$$q_e = \frac{q_{\max} K_L C_e}{1 + K_L C_e} \quad (3)$$

where: q_{\max} = maximum sorption capacity (mg·g⁻¹), C_e = denotes the contaminant concentration at equilibrium (mg·dm⁻³), K_L = Langmuir constant that indicates the affinity between the adsorbent and the adsorbate (dm³·mg⁻¹).

Sorption kinetics model was also analysed. The sorption kinetic models included the first-order pseudo model, the second-order pseudo model, and the intra particle diffusion model, represented by Equations (4), (5), and (6), respectively.

$$q_t = q_e [1 - \exp(-K_{1p}t)] \quad (4)$$

where: q_t = sorption capacity at a given time t (mg·g⁻¹), K_{1p} = first-order pseudo constant (h⁻¹), and t = contact time (h).

$$q_t = \frac{K_{2p} q_e^2 t}{1 + K_{2p} q_e^2 t} \quad (5)$$

where: K_{2p} = second-order pseudo rate constant (g·mg⁻¹·h⁻¹).

$$q_t = K_p t^{0.5} + C \quad (6)$$

where: K_p = intra-particle diffusion rate constant ($\text{mg}\cdot\text{g}^{-1}\cdot\text{h}^{-0.5}$), C = a constant to the boundary layer thickness (unitless).

FIXED BED COLUMN STUDY

A continuous flow experiment using a fixed-bed reactor was carried out using locally available coconut shell biochar (CST). The coconut shell biochar was produced at a pyrolysis temperature of 300°C , with particle size of ~ 1 cm, bulk density of $0.17\text{ g}\cdot\text{cm}^{-3}$, particle density of $1.034\text{ g}\cdot\text{cm}^{-3}$, and porosity of 50%. The column used was 20 cm high and internal diameter of 5 cm. The real agricultural wastewater was used as the influent, collected from an intensive agricultural area in Solok Regency, West Sumatera Province, Indonesia. The hydraulic loading rate was set at $30\text{ cm}^3\cdot\text{min}^{-1}$. Observations were performed over 24 h, recorded every 30 min during the first 2 h, every hour up to 5 h, and then every 3 h. This experiment was conducted at ambient temperature.

The breakthrough model in the adsorption column experiment used the Thomas model, Adam and Bohart model, and Yoon–Nelson model respectively using the formulas presented in Equations (6), (7), and (8) (Nguyen, 2015; Patel, 2020).

$$\ln\left(\frac{C_0}{C_t} - 1\right) = K_{TH} q_0 \frac{m}{Q} - K_{TH} C_0 t \quad (7)$$

where: K_{TH} = Thomas constant ($\text{cm}^3\cdot\text{min}^{-1}\cdot\text{mg}^{-1}$), q_0 = adsorption capacity ($\text{mg}\cdot\text{g}^{-1}$), m = sorbent mass (g), Q = flow rate ($\text{cm}^3\cdot\text{min}^{-1}$), t = contact time (min), C_0 = inlet concentration ($\text{mg}\cdot\text{dm}^{-3}$), C_t = outlet concentration at time t ($\text{mg}\cdot\text{dm}^{-3}$).

$$\ln\left(\frac{C_0}{C_t} - 1\right) = K_{AB} N_0 \frac{Z}{u} - K_{AB} C_t t \quad (8)$$

where: K_{AB} = Adam Bohart constant ($\text{dm}^3\cdot\text{mg}^{-1}\cdot\text{min}^{-1}$), N_0 = column saturation concentration ($\text{mg}\cdot\text{dm}^{-3}$), Z = depth (cm), u ($\text{cm}\cdot\text{min}^{-1}$) = linear velocity achieved by dividing the flow rate ($\text{cm}^3\cdot\text{min}^{-1}$) by the column cross-sectional area (cm^2).

$$\ln \frac{C}{C_0 - C} = K_{YN} t - K_{YN} \tau \quad (9)$$

where: t = contact time (min), τ = time required to reach 50% breakthrough time (min), K_{YN} = Yoon–Nelson constant (min^{-1}).

RESULTS AND DISCUSSION

PHYSICAL CHARACTERISTICS OF THE MEDIA

The scanning electron microscope images show the number of pores on the surface of coconut shell biochar increases with the increase of pyrolysis temperatures (Fig. 1a–d). Coconut shell biochar made at higher pyrolysis temperatures is more porous than biochar produced at lower temperatures. Higher pyrolysis temperatures are linked to notable changes in the surface area and porosity of biochar. This occurs due to the breakdown of organic material and the development of micropores. At elevated pyrolysis temperatures, volatile compounds in the biomass decompose more thoroughly, resulting in a carbon structure with increased porosity. Additionally, higher temperatures impact the surface area of biochar by removing or thermally breaking down substances that block pores, thereby improving the

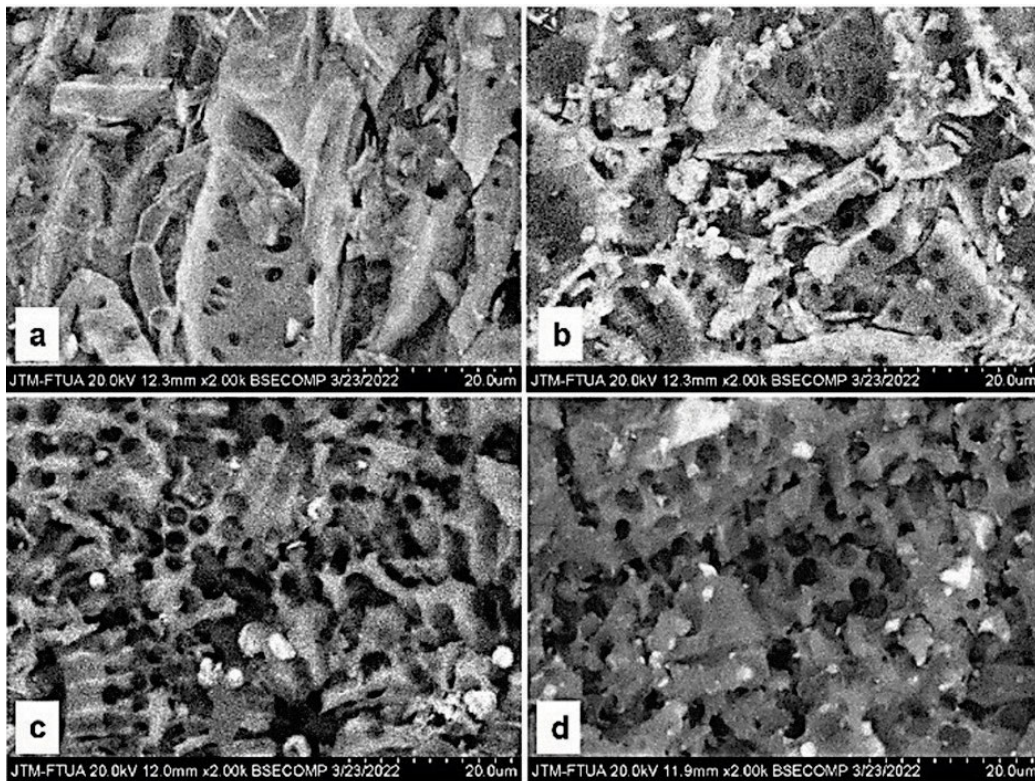


Fig. 1. Surface morphology of coconut shell biochar: a) CS300 (pyrolysis temperature = 300°C), b) CS450 (pyrolysis temperature = 450°C), c) CS600 (pyrolysis temperature = 600°C), d) CST (local biochar); source: own study

accessibility of the biochar's external surface (Tomczyk, Sokolowska and Boguta, 2020). The increased number and size of pores on the surface of biochar contributes to the greater number of sorption sites.

The results of the EDX analysis in Figure 2 demonstrate that the carbon level also increases with the higher pyrolysis temperature of biochar. Carbon is the main element that is presents in biochar because it is made from the heating process. In addition to carbon, oxygen is also present, but it decreases with the higher pyrolysis temperature. This decrease is due to dehydration processes and the release of volatile compounds that contain oxygen (Dhar, Sakib and Hilary, 2022). Likewise, potassium levels were detected in biochar which also decreased with the increasing of pyrolysis temperature. Potassium is one of elements in raw coconut shells (Leman *et al.*, 2017; Suman and Gautam, 2017). As the pyrolysis temperature rises, the complex-potassium and graphite layer-potassium in coconut shell biochar start to break down, leading to a reduced potassium concentration by the end of the process (Dissanayaka *et al.*, 2023).

The analysis of FTIR in Figure 3 reveals that various spectra are present in the local biochar, including -OH stretching ($3,500\text{--}3,200\text{ cm}^{-1}$), aromatic C=C and C=O of conjugated ketones and quinones ($1,613\text{ cm}^{-1}$), and C-O-C ($1,049\text{ cm}^{-1}$). These functional groups play a crucial role in nutrient sorption through ion exchange mechanisms (Janu *et al.*, 2021). Functional groups, such as hydroxyl, carboxyl groups, and phenol along with and

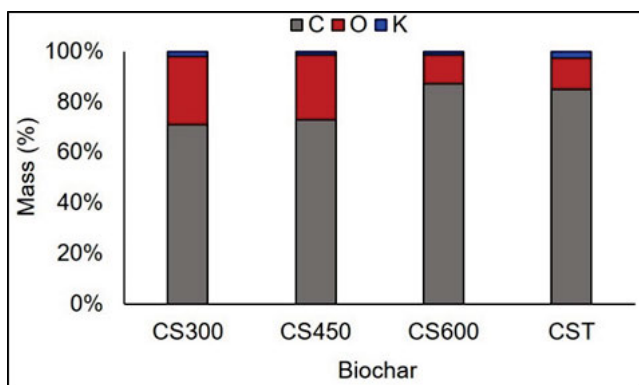


Fig. 2. EDX analysis of coconut shell biochar; CS300, CS450, CS600, and CST as in Fig. 1; source: own study

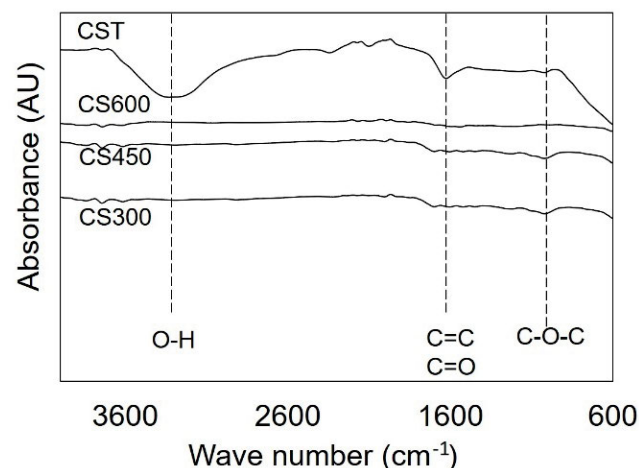


Fig. 3. Biochar functional groups of biochar CS300, CS450, CS600, and CST; CS300, CS450, CS600, and CST as in Fig. 1; source: own study

basic functional groups like pyridine, aromatic amines, and amides, serve as anion and cation exchange sites for ammonium, nitrate, and phosphate (Wang *et al.*, 2015, Yin *et al.*, 2017). Furthermore, Zeng *et al.* (2018) found that aliphatic C-O-C, C=O, and C=C, and functional groups were depleted from the biochar ammonium adsorption (Wei *et al.*, 2018) suggesting that these functional groups actively participate in binding with ammonium ions present in wastewater.

BIOCHAR SORPTION CAPACITY

In this study, the dissolved oxygen (DO) and pH of the wastewater solution in each experimental variation were measured. This helps to understand the interactions between biochar and pollutants, and provides insights into how biochar affects the physicochemical parameters of water. DO in the solution at the end of the experiment using coconut shell biochar variations ranged from $4.30\text{ to }5.60\text{ mg}\cdot\text{dm}^{-3}$, from $4.50\text{ to }5.10\text{ mg}\cdot\text{dm}^{-3}$, and from $4.60\text{ to }5.40\text{ mg}\cdot\text{dm}^{-3}$, respectively.

Based on the maximum sorption capacity calculations presented in Table 1, the maximum sorption capacity of ammonium, nitrate, and phosphate by biochar increases with higher pyrolysis temperatures. This is closely related to the greater number of pores in biochar produced at higher pyrolysis temperatures, as presented in Figure 1. The sorption capacity of ammonium and phosphate show that the local biochar (slow pyrolysis 300°C with traditional method using barrel) is comparable to the sorption capacity of biochar produced at a higher pyrolysis temperature (CS600), while the sorption capacity of nitrate is close to the sorption ability of biochar

Table 1. Sorption capacity and isotherm of each biochar variation

Biochar	Q_{\max} ($\text{mg}\cdot\text{g}^{-1}$)	Langmuir		Freundlich		
		K_L	R^2	n	K_F	R^2
Ammonium						
CS300	9.95	0.13	0.91	1.37	1.15	0.94
CS450	9.81	0.16	0.95	1.46	1.31	0.98
CS600	10.29	0,12	0.97	1.45	1.17	0.99
CST	10.12	0,13	0.96	1.46	1.52	0.99
Nitrate						
CS300	4.13	0.05	0.77	0.87	0.29	0.34
CS450	7.21	0.16	0.78	1.29	0.86	0.80
CS600	15.49	0.03	0.83	0.88	0.28	0.83
CST	7.51	0.11	0.73	1.13	0.32	0.73
Phosphate						
CS300	6.62	0.42	0.74	1.77	1.78	0.77
CS450	7.25	0.21	0.80	1.35	1.05	0.82
CS600	8.54	0.14	0.91	1.52	1.15	0.76
CST	8.85	0.13	0.68	1.34	1.28	0.42

Explanations: q_{\max} = maximum flow rate ($\text{mg}\cdot\text{g}^{-1}$), K_L = Langmuir constant, K_F = Freundlich constant, R^2 = determination coefficient, CS300, CS450, CS600, and CST as in Fig. 1.

Source: own study.

CS450. Observations also show that the pores of local biochar closely resemble those of biochar made at a pyrolysis temperature of 600°C (Fig. 1).

The effect of pyrolysis temperature on ammonium sorption capacity in this study is similar to the research carried out by Zou *et al.* (2022), who used coconut shell biochar prepared at higher pyrolysis temperature of 600°C. This performance was inversely proportional to the ammonium removal using corn cob biochar as developed by Liu *et al.* (2014) and Gai *et al.* (2014), who obtained higher ammonium adsorption capacity with biochar made at a lower pyrolysis temperature.

The study using date palm biochar prepared at 700°C demonstrated a higher adsorption capacity for nitrate removal (Alsewaileh, Usman and Al-Wabel, 2019), showing the same trend to the nitrate removal using coconut shell biochar in the present study. However, coconut shell biochar prepared with pyrolysis at 300°C by Zou *et al.* (2022) exhibited a higher nitrate adsorption capacity compared to this study. Similarly, rice husk biochar showed greater sorption capacity compared to coconut shell (CS) biochar (Konneh *et al.*, 2021; Zou *et al.*, 2022; Edwin *et al.*, 2023b). Overall, the performance of CS biochar prepared in this study is comparable to that of biochars derived from different sources reported in previous studies.

The trend of phosphate removal in this study mirrors that of ammonium removal, with higher phosphate sorption capacity observed in biochar produced at lower pyrolysis temperatures. The presence of potassium in biochar can enhance phosphate adsorption, and potassium content is typically higher in coconut shell biochar produced at lower pyrolysis temperatures. Additionally, biochar produced at lower temperatures exhibits a higher cation exchange capacity (CEC), contributing to greater ammonium and phosphate adsorption. Similar findings were reported by Gai *et al.* (2014), who observed that biochar produced at lower pyrolysis temperatures of 400°C and 500°C exhibited a higher cation exchange capacity than biochar produced at higher temperatures of 600°C and 700°C (Gai *et al.*, 2014).

Several factors can affect the sorption of ammonium, nitrate, and phosphate, including the type of sorbent material, concentration of contaminants in water, pyrolysis temperature, pH, and any modifications to the sorbent (Fidel, Laird and

Spokas, 2018). Pyrolysis temperature affects the surface area of biochar, which serves as the primary site for contaminants sorption. This is due to the release of volatile substances from the biomass structure; however, at excessively high pyrolysis temperatures, biochar surface pores may become clogged (Yin *et al.*, 2018). Jung *et al.* (2015) reported a positive correlation between surface area and nutrient adsorption, which is consistent with the nutrient removal trend using coconut shell biochar in this study. Pyrolysis temperature also significantly influences both type and quantity of functional groups as well as the cation exchange capacity of biochar. The effect of biochar functional groups on the sorption of phosphate is comparable to their role in nitrate sorption, due to the anionic nature of both nutrients. However, only limited number of studies have thoroughly explored and confirmed this relationship (Yin *et al.*, 2018).

SORPTION ISOTHERM AND KINETIC

In isotherm analysis, the model with the R^2 value closest to 1 is considered the best fit for describing the adsorption process. As shown in Table 1, the R^2 values for ammonium sorption using all variations of biochar indicate that both the Langmuir and Freundlich isotherms provide a good fit. The Langmuir isotherm describes a monolayer-sorption process, where sorption occurs on a finite number of distinct sorption sites. Each site can adsorb only one molecule, all sites are energetically equivalent, and there is no interaction between adsorbed molecules (Kumar *et al.*, 2010).

In contrast, the Freundlich isotherm describes non-ideal sorption, involving multi-layer adsorption on heterogeneous surfaces. It assumes that sorption occurs at multiple sites with varying energy levels, where the most active binding sites being occupied first (Nguyen, 2015).

The best-fitting sorption kinetics model is identified by the highest the R^2 value, closest to 1. As shown in Table 2, the CST align best with the intra particle diffusion model. For nitrate removal, coconut shell biochar made at 300°C (CS300) and 450°C (CS450) are better described by the second-order pseudo kinetic model, while biochar made at 600°C pyrolysis temperature and local biochar are more accurately described by the intra-particle

Table 2. Sorption kinetic of coconut shell biochar

Material	Pseudo 1 st order			Pseudo 2 nd order			Intra particle diffusion		
	K_{1p}	q_e	R^2	K_{2p}	q_e	R^2	K_p	C	R^2
Ammonium removal									
CS300	0.72	2.14	0.80	0.16	2.48	0.65	1.21	0.39	0.88
CS450	0.66	1.49	0.66	0.08	2.96	0.47	1.09	0.71	0.75
CS600	0.61	1.80	0.72	0.09	2.91	0.52	1.09	0.61	0.79
CST	0.76	2.40	0.89	0.15	2.42	0.66	1.23	0.44	0.90
Nitrate removal									
CS300	0.89	4.24	0.85	3.66	2.07	1.00	1.19	0.34	0.92
CS450	1.48	7.08	0.67	1.92	1.84	0.94	1.29	0.51	0.80
CS600	1.12	3.77	0.92	0.33	2.10	0.88	1.29	0.10	0.98
CST	1.61	3.01	0.96	0.17	2.24	0.68	1.32	0.43	0.91

cont. Tab. 2

Material	Pseudo 1 st order			Pseudo 2 nd order			Intra particle diffusion		
	K_{1p}	q_e	R^2	K_{2p}	q_e	R^2	K_p	C	R^2
Phosphate removal									
CS300	0.46	2.26	0.75	0.10	3.07	0.58	1.00	0.49	0.83
CS450	0.44	2.75	0.84	0.14	2.92	0.70	0.99	0.33	0.89
CS600	0.26	2.34	0.58	0.06	4.20	0.51	0.75	0.45	0.77
CST	0.53	2.66	0.84	0.25	2.27	0.80	1.21	0.21	0.92

Explanations: K_{1p} = first-order pseudo constant (h^{-1}), q_e = quantity of nutrients adsorbed per gram of the adsorbent at equilibrium ($\text{mg}\cdot\text{g}^{-1}$), R^2 = determination coefficient, K_{2p} = second-order pseudo rate constant ($\text{g}\cdot\text{mg}^{-1}\cdot\text{h}^{-1}$), C = a constant to the boundary layer thickness (unitless), K_p = the intra-particle diffusion rate constant ($\text{mg}\cdot\text{g}^{-1}\cdot\text{h}^{-0.5}$), CS300, CS450, CS600, and CST as in Fig. 1.

Source: own study.

diffusion and the first-order pseudo model. For phosphate removal, the intra-particle diffusion model provides the best fit for the sorption kinetics of the local biochar.

The intra-particle diffusion model describes sorption as involving four steps, including migration of contaminant molecules from the solution to the sorption material surface, diffusion through the boundary layer to the sorption material surface, and intra-particle diffusion into the interior of the sorption material (Yagub *et al.*, 2014). The second-order pseudo model illustrates that the sorption rate is proportional to the increasing available sites which decreases as the equilibrium state is approached. This model indicates a strong interaction between contaminant and sorption material. This model also indicates the possibility of chemical sorption mechanisms in experiments involving ion exchange processes between adsorbents and contaminants. In contrast, the first-order pseudo model describes sorption as a process where the rate is proportional to the number of unoccupied sites at a given time (Zhou *et al.*, 2019; Wang and Guo, 2020).

FIXED BED COLUMN STUDY

In this study, a fixed bed column experiment was performed to further analyse the nutrient sorption capacity using coconut shell biochar. The initial concentration of ammonium, nitrate, and phosphate in agricultural wastewater were $5.445 \text{ mg}\cdot\text{dm}^{-3}$, $7.543 \text{ mg}\cdot\text{dm}^{-3}$, and $5.750 \text{ mg}\cdot\text{dm}^{-3}$, respectively. The retention time of wastewater in the column was 6.54 min. The ratio of effluent and initial concentration of contaminant is presented in Figure 4. The initial pH, dissolved oxygen, and temperature were 6.83,

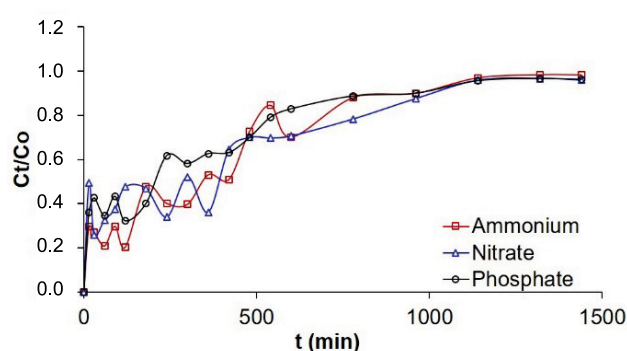


Fig. 4. Removal of ammonium, nitrate, and phosphate and the removal efficiency using a continuous column experiment; t = time, C_t = outlet concentration, C_0 = inlet concentration; source: own study

$7.4 \text{ mg}\cdot\text{dm}^{-3}$, and 24.4°C , respectively. The removal efficiency for ammonium, nitrate, and phosphate ranged 20.3–98.3%, 25.8–96.6%, and 32.2–96.5%, respectively.

As shown in Table 3, the Thomas model was identified as the most accurate for describing nutrient removal in this study. The Thomas model assumes that sorption is primarily governed by mass transfer at the interface rather than chemical interactions, aligning well with the Langmuir isotherm and second-order pseudo kinetic models (Patel, 2020). This model effectively captures the overall breakthrough curve for the sorption process. According to the model calculations, the sorption rate was found to be highest for ammonium, followed by phosphate, and then nitrate, indicating the varying effectiveness of the biochar in removing these nutrients.

Table 3. Breakthrough model for nutrient removal using fixed bed column

Parameter	Adam Bohart model			Thomas model			Yoon–Nelson model		
	K_{AB}	N_0	R^2	K_{TH}	q_0	R^2	K_{YN}	τ	R^2
Ammonium	$1.1\cdot 10^{-4}$	11.89	0.24	$5.4\cdot 10^{-4}$	0.47	0.89	$2.0\cdot 10^{-3}$	95.44	0.67
Nitrate	$6.2\cdot 10^{-5}$	23.20	0.16	$2.1\cdot 10^{-4}$	1.19	0.71	$6.0\cdot 10^{-4}$	92.83	0.15
Phosphate	$8.1\cdot 10^{-5}$	13.25	0.22	$5.2\cdot 10^{-4}$	0.43	0.90	$1.7\cdot 10^{-3}$	123.52	0.75

Explanations: K_{AB} = Adam Bohart constant ($\text{dm}^3\cdot\text{mg}^{-1}\cdot\text{min}^{-1}$), N_0 = column saturation concentration ($\text{mg}\cdot\text{dm}^{-3}$), R^2 = determination coefficient, q_0 = adsorption capacity ($\text{mg}\cdot\text{g}^{-1}$), K_{TH} = Thomas constant ($\text{cm}^3\cdot\text{min}^{-1}\cdot\text{mg}^{-1}$), K_{YN} = Yoon–Nelson constant (min^{-1}), τ = time required to reach 50% breakthrough time (min).

Source: own study.

CONCLUSIONS

Studies have shown that biochar is effective in removing contaminants such as nutrients from wastewater. The utilisation of widely available material is important as a sustainable approach for the environment. Coconut shell waste, which is abundant in tropical countries, is a potential resource for biochar production. The sorption capacity of coconut shell biochar in removing nitrate, ammonium, and phosphate from agricultural wastewater was examined in the laboratory in batch and column experiments. Pyrolysis temperature affects the removal efficiency of ammonium, nitrate, and phosphate by biochar. This study found that biochar produced at higher pyrolysis temperatures exhibited greater sorption capacities, indicating the critical role of surface area in enhancing nutrient removal performance. In this study, in addition to morphological structure of biochar, the presence of specific functional groups also affected nutrient sorption capacity of biochar. The fixed-bed column experiment further confirmed the potential of biochar in removing nutrients from agricultural wastewater. These findings highlight the potential of coconut shell biochar as an eco-friendly and efficient alternative for nutrient removal from agricultural wastewater.

ACKNOWLEDGEMENT

The authors would acknowledge Lembaga Penelitian dan Pengabdian kepada Masyarakat (LPPM) of Universitas Andalas for the publications funding.

CONFLICTS OF INTEREST

All authors declare that they have no conflict of interests.

REFERENCES

- Alsewaleh, A.S., Usman, A.R. and Al-Wabel, M.I. (2019) "Effects of pyrolysis temperature on nitrate-nitrogen (NO_3^- -N) and bromate (BrO_3^-) adsorption onto date palm biochar," *Journal of Environmental Management*, 237, pp. 289–296. Available at: <https://doi.org/10.1016/j.jenvman.2019.02.045>.
- American Public Health Association (APHA), American Water Works Association (AWWA), & Water Environment Federation (WEF) (2003) *Standard methods for the examination of water and wastewater* (23rd edn). APHA.
- Dhar, S.A., Sakib, T.U. and Hilary, L.N. (2022) "Effects of pyrolysis temperature on production and physicochemical characterization of biochar derived from coconut fiber biomass through slow pyrolysis process," *Biomass Conversion and Biorefinery*, 12(7), pp. 2631–2647. Available at: <https://doi.org/10.1007/s13399-020-01116-y>.
- Dissanayaka, D.M.N.S. et al. (2023) "Effects of pyrolysis temperature on chemical composition of coconut-husk biochar for agricultural applications: a characterization study," *Technology in Agronomy*, 3, 13. Available at: <https://doi.org/10.48130/tia-2023-0013>.
- Edwin, T. et al. (2023a) "A multivariate approach to the water quality environment of a tropical lake surrounded by agricultural land," *Water Practice and Technology*, 18(5), pp. 1209–1220. Available at: <https://doi.org/10.2166/wpt.2023.058>.
- Edwin, T. et al. (2023b) "Impact of pyrolysis temperature on the removal of nutrients using coarse rice-husk biochar," *Journal of Ecological Engineering*, 24(12), pp. 247–257. Available at: <https://doi.org/10.12911/22998993/173379>.
- Fidel, R.B., Laird, D.A. and Spokas, K.A. (2018) "Sorption of ammonium and nitrate to biochars is electrostatic and pH-dependent," *Scientific Reports*, 8(1), 17627. Available at: <https://doi.org/10.1038/s41598-018-35534-w>.
- Gai, X. et al. (2014) "Effects of feedstock and pyrolysis temperature on biochar adsorption of ammonium and nitrate," *PLoS ONE*, 9(12), 113888. Available at: <https://doi.org/10.1371/journal.pone.0113888>.
- Janu, R. et al. (2021). "Biochar surface functional groups as affected by biomass feedstock, biochar composition and pyrolysis temperature," *Carbon Resources Conversion*, 4(January), pp. 36–46. Available at: <https://doi.org/10.1016/j.crcon.2021.01.003>.
- Jung, K.W. et al. (2015) "Kinetic study on phosphate removal from aqueous solution by biochar derived from peanut shell as renewable adsorptive media," *International Journal of Environmental Science and Technology*, 12(10), pp. 3363–3372. Available at: <https://doi.org/10.1007/s13762-015-0766-5>.
- Komala, P.S. et al. (2023) "Spatio-temporal changes of water quality based on water quality index method in tropical lake of Indonesia," *Water, Air, and Soil Pollution*, 234(9), 594. Available at: <https://doi.org/10.1007/s11270-023-06599-9>.
- Konneh, M. et al. (2021) "Adsorption and desorption of nutrients from abattoir wastewater: Modelling and comparison of rice, coconut and coffee husk biochar," *Heliyon*, 7(11), e08458. Available at: <https://doi.org/10.1016/j.heliyon.2021.e08458>.
- Kumar, A. and Bhattacharya, T. (2021) "Biochar: A sustainable solution, environment, development and sustainability," *Environment, Development and Sustainability*, 23, pp. 6642–6680. Available at: <https://doi.org/10.1007/s10668-020-00970-0>.
- Kumar, P. et al. (2010) "Phosphate removal from aqueous solution using coir-pith activated carbon," *Separation Science and Technology*, 45(10), pp. 1463–1470. Available at: <https://doi.org/10.1080/01496395.2010.485604>.
- Leman, A.M. et al. (2017) "The effect of activation agent on surface morphology, density and porosity of palm shell and coconut shell activated carbon," *AIP Conference Proceedings*, 1885, 020001. Available at: <https://doi.org/10.1063/1.5002195>.
- Liu, X. et al. (2014) "Characterization of corncob-derived biochar and pyrolysis kinetics in comparison with corn stalk and sawdust," *Bioresourcel Technology*, 170, pp. 76–82. Available at: <https://doi.org/10.1016/j.biortech.2014.07.077>.
- Nguyen, T.A.H. (2015) *Removal and recovery of phosphorus from municipal wastewater by adsorption coupled with crystallization*. PhD Thesis. Sydney, Australia: University of Technology. Available at: <https://opus.lib.uts.edu.au/handle/10453/38985> (Accessed: April 3, 2024).
- Patel, H. (2020) "Batch and continuous fixed bed adsorption of heavy metals removal using activated charcoal from neem (*Azadirachta indica*) leaf powder," *Scientific Reports*, 10(1), pp. 1–12. Available at: <https://doi.org/10.1038/s41598-020-72583-6>.
- Rosemarin, A. et al. (2020) "Circular nutrient solutions for agriculture and wastewater – a review of technologies and practices," *Current Opinion in Environmental Sustainability*, 45, pp. 78–91. Available at: <https://doi.org/10.1016/j.cosust.2020.09.007>.
- Suman, S. and Gautam, S. (2017) "Pyrolysis of coconut husk biomass: Analysis of its biochar properties," *Energy Sources, Part A: Recovery, Utilization and Environmental Effects*, 39(8), pp. 761–767. Available at: <https://doi.org/10.1080/15567036.2016.1263252>.

- Tchobanoglous, G., Burton, F.L. and Stensel, D. (2003) *Wastewater engineering: Treatment, disposal, reuse*. 4th edn. Hong Kong: Metcalf & Eddy, Inc. Boston: McGraw-Hill, Inc.
- Tomczyk, A., Sokołowska, Z. and Boguta, P. (2020) "Biochar physicochemical properties: pyrolysis temperature and feedstock kind effects," *Reviews in Environmental Science and Biotechnology*, 19(1), pp. 191–215. Available at: <https://doi.org/10.1007/s11157-020-09523-3>.
- Wang, J. and Guo, X. (2020) "Adsorption kinetic models: Physical meanings, applications, and solving methods," *Journal of Hazardous Materials*, 390, 122156. Available at: <https://doi.org/10.1016/j.jhazmat.2020.122156>.
- Wang, Z. et al. (2015) "Biochar produced from oak sawdust by lanthanum (La)-involved pyrolysis for adsorption of ammonium (NH_4^+), nitrate (NO_3^-), and phosphate (PO_4^{3-})," *Chemosphere*, 119, 646–653. Available at: <https://doi.org/10.1016/j.chemosphere.2014.07.084>.
- Wei, D. et al. (2018) "Biochar-based functional materials in the purification of agricultural wastewater: Fabrication, application and future research needs," *Chemosphere*, 197, pp. 165–180. Available at: <https://doi.org/10.1016/j.chemosphere.2017.12.193>.
- Yagub, M.T. et al. (2014) "Dye and its removal from aqueous solution by adsorption: A review," *Advances in Colloid and Interface Science*, 209, pp. 172–184. Available at: <https://doi.org/10.1016/j.cis.2014.04.002>.
- Yin, Q. et al. (2017) "Biochar as an adsorbent for inorganic nitrogen and phosphorus removal from water: A review," *Environmental Science and Pollution Research*, 24(34), pp. 26297–26309. Available at: <https://doi.org/10.1007/s11356-017-0338-y>.
- Yin, Q. et al. (2018) "Evaluation of nitrate and phosphate adsorption on Al-modified biochar: Influence of Al content," *Science of the Total Environment*, 631–632, pp. 895–903. Available at: <https://doi.org/10.1016/j.scitotenv.2018.03.091>.
- Zhou, L. et al. (2019) "Phosphorus and nitrogen adsorption capacities of biochars derived from feedstocks at different pyrolysis temperatures," *Water*, 11(8), pp. 1–16. Available at: <https://doi.org/10.3390/w11081559>.
- Zou, G. et al. (2022) "Comparative effectiveness of biochar derived from tropical feedstocks on the adsorption for ammonium, nitrate and phosphate," *Archives of Environmental Protection*, 48(4), pp. 25–34. Available at: <https://doi.org/10.24425/aep.2022.143706>.